J Herbmed Pharmacol. 2023; 12(2): 241-249.

http://www.herbmedpharmacol.com doi: 10.34172/jhp.2023.26

Journal of Herbmed Pharmacology

Co-administration of herbal inhibitors of P-glycoprotein with renal drugs enhance their bioavailability – *In silico* approach

Chandana Roy, **Pratiti Ghosh***

Department of Physiology, West Bengal State University, Kolkata-700126, India

ARTICLE INFO

Article Type:
Original Article

Article History:
Received: 29 November 2022
Accepted: 27 January 2023

Keywords:
Multidrug resistance
Efflux transporter
Biological availability
Herbs
Docking

ABSTRACT

Introduction: Multidrug resistance (MDR) is primarily associated with reduced intracellular drug accumulation owing to overexpression of p-glycoprotein, an active efflux transporter. Competitive inhibition or allosteric modulation of p-glycoprotein may alter the pharmacokinetics of the drugs that serve as substrates, resulting in enhanced drug bioavailability and tissue penetration. This study endeavors to assess the efficacy of the components of reno-protective herbs in the inhibition of p-glycoprotein activity thereby enhancing the possibility of the retention of co-administered renal medications inside the target cells.

Methods: Drug-likeness and pharmacokinetic properties were determined to ensure the safety and efficacy of herbal constituents. Molecular docking employing the CDOCKER module of Discovery Studio was performed to investigate the binding affinity between the active constituents and the p-glycoprotein receptor (6C0V). Molecular dynamics simulation was utilized to further assess the stability of the complex of receptors with the component bearing its maximal affinity.

Results: The analyses suggested that the inhibitors viz., atisine, kutkin, and embelin from *Aconitum heterophyllum,* phylloquinone from *Calendula officinalis*, stigmasterol from *Paederia foetida*, and convallamarogenin from *Convallaria majalis* demonstrated maximum binding affinity towards p-glycoprotein.

Conclusion: Atisine may thus be identified as the lead compound in the augmentation of drug bioavailability inside the cell, along with its reno-protective efficacy.

Implication for health policy/practice/research/medical education:
Renal drug efflux by p-glycoprotein has been a major hurdle in its bioavailability, which may be circumvented by screening for its natural reno-protective nontoxic inhibitors, viz., atisine, embelin, phylloquinone, or stigmasterol which may be synergistically administered with the treatment drugs to alleviate the disease.

Please cite this paper as: Roy C, Ghosh P. Co-administration of herbal inhibitors of P-glycoprotein with renal drugs enhance their bioavailability – *In silico* approach. J Herbmed Pharmacol. 2023;12(2):241-249. doi: 10.34172/jhp.2023.26.

Introduction

Drug efflux transporters such as p-glycoprotein play a major role in the maintenance of cellular homeostasis and are primarily responsible for multidrug resistance (MDR). P-glycoprotein is ubiquitously expressed in the epithelial cells of the small intestine, liver, kidney, and endothelial cells of the blood-brain barrier to expel the toxic compounds but in the process also modulates the pharmacodynamics of the drugs. So, the identification and formulation of p-glycoprotein inhibitors, which when co-administered with such drugs, is a strategy that would enhance drug bioavailability inside the target cells (1).

The beneficial effects of medicinal plants on kidney dysfunction are often attributed to their antioxidant defense mechanisms with additive benefits on inflammation and fibrosis (2). Furthermore, some plants and their active metabolites are known to ameliorate kidney ailments such as interstitial nephritis, altered intraglomerular hemodynamics, and glomerulonephritis (3). These bioactive ingredients have functional scaffolds to revert p-glycoprotein-mediated MDR (4). The majority of renal drugs viz., cyclosporine (5), mycophenolate (6), tacrolimus (7), dapagliflozin (8), and valsartan (9) are substrates of p-glycoprotein and are thus effluxed by the cells.

Here, twenty-seven plants with renal proficiency viz., *Sida rhombifolia* (10), *Apium leptophyllum* (11), *Aconitum heterophyllum* (12), *Abies webbiana* (13), *Artocarpus*

***Corresponding author**: Pratiti Ghosh, Email: pratitig@wbsu.ac.in

hirsutus (14), *Paederia foetida* (15), *Cocculus pendulus* (16), *Alangium salvifolium* (17), *Ruta graveolens* (18), *Calophyllum inophyllum* (19), *Rubia cordifolia* (20), *Myrtus communis* (21), *Pongamia pinnata* (22), *Convallaria majalis* (23), *Saussurea costus* (24), *Mimusops elengi* (25), *Calendula officinalis* (26), *Ficus bengalensis* (27), *Hypericum mysorense* (28), *Toona sinensis* (29), *Nelumbo nucifera* (30), *Chelidonium majus* (31), *Eclipta alba* (32), *Alstonia scholaris* (33), *Pterocarpus marsupium* (34), *Centella asiatica* (35), and *Plumbago zeylanica* (36) have been chosen to screen their inhibitory binding efficacy with the efflux transporter by molecular docking. This study will help in the identification of reno-protective natural compounds as p-glycoprotein inhibitors, which in addition possess the ability to enhance the absorption of renal treatment substrate drugs inside the efflux-prone target cell.

Materials and Methods

Protein preparation

The 3D crystal structure of p-glycoprotein (PDB code: 6C0V) used for the docking evaluation was downloaded from the protein data bank (http://www.rcsb.org) at a resolution of about 3.4 Å (37). The protein was energetically minimized using the protein preparation wizard of Discovery Studio. This involved the cleaning of protein and optimization of side-chain conformations using the ChiRotor algorithm. The potential binding pockets were detected using Dogsitescorer server (https://proteins.plus/#dogsite).

Ligand preparation

3D structures and canonical smiles of 376 ligand molecules (Table S1) and control drugs doxycycline and elacridar, were obtained for molecular docking from PubChem (https://pubchem.ncbi.nlm.nih.gov/), chEMBL (https://www.ebi.ac.uk/chembl/), and ChemSpider (http://www.chemspider.com/) databases. The canonical SMILES were translated into SDF files employing the online SMILE translator (https://cactus.nci.nih.gov/translate/). The prepare ligands protocol of discovery studio was used to perform tasks such as the removal of duplicates and computing isomers and tautomers.

Drug likeness and ADMET analysis

Druggability of the components were examined with Molinspiration tool (http://www.molinspiration.com). Pharmacokinetic study was performed with the pkCSM tool to examine the ADMET (Absorption, Distribution, Metabolism, Excretion, and Toxicity) property of the small molecules (http://biosig.unimelb.edu.au/pkcsm/prediction).

Molecular docking analysis

The receptor-ligand docking evaluation was performed by the CDOCKER module of Discovery Studio (version 2019 onwards) which is based on CHARMm-based docking algorithm. The ligands were flexed with the rigid receptor during the refinement and high-temperature dynamics generated random ligand conformations which were refined by grid-based (GRID1) simulated annealing and forcefield minimization. A set of refined ligand poses for each component was generated and the best pose was selected on the basis of the lowest binding free energy.

The design of the experiment was aimed towards a ligand-based approach, thus allowing the incorporation of all the binding poses for all the ligands used in the study. This maximized the pool of proposed hits which could develop into lead compounds.

Molecular dynamics simulation

The top-scoring conformation identified through docking analyses was used for molecular dynamics (MD) simulation. The ligand-receptor complex was subjected to CHARMm36 force-field and the solvation was performed under Explicit Periodic Boundary conditions. The system was relaxed by two rounds of energy minimization (500 steps of steepest descent and 500 steps of conjugate gradient) with the final RMS gradient of 0.1. The temperature of the system was raised from 50 K to 300 K (heating) for 4ps and equilibration was performed for 10ps. The simulation (production) was executed for 10ps with a time step of 2fs at a constant temperature of 300 K. The electrostatic calculation was set to particle mesh Ewald (PME) and Verlet leapfrog integrator (LEAP) was used to perform numerical integration of the equation of motion. The analyze trajectory protocol was employed to calculate geometric properties such as distance, angle, torsion, and the number of non-bond interactions for each simulation frame. Root mean square fluctuation (RMSF) from the average structure in the trajectory and interaction energy between two sets of atoms were also computed. The stability of the conformation was assessed through binding free energy calculation using Poisson-Boltzmann with non-polar surface area (PBSA) method and radius of gyration (Rg).

Results

A total of 376 components of 27 reno-protective herbs were initially screened on the basis of druggability and ADMET properties. These were then docked against outward facing p-glycoprotein transporter, 6C0V. Considering substrate *expulsion* from an inward V-shaped transmembrane receptor, the outward-facing conformation is necessary for the study of the more exposed inhibitor-binding and substrate-binding domains. P-glycoprotein uses the energy from ATP hydrolysis to extrude drug substrates out of the cell, locking it in outward V conformation when another ATP hydrolysis reverses it to the unbound inward V conformation.

Drug-likeness

Drug-likeness result was computed based on Lipinski's

rule of five (38), which showed that 331 compounds had acceptable drug-like properties indicating a good oral bioavailability (Table 1).

ADMET prediction

The ADMET properties were computed using pkCSM revealing that 39 components served as p-glycoprotein inhibitors and their ADMET values were within an acceptable range (Table 2). ADMET features affect oral bioavailability and metabolism of small molecules (39).

Molecular docking analysis

To understand the binding interaction of herbal components with p-glycoprotein, molecular docking analysis was conducted using Discovery Studio. The p-glycoprotein inhibitors were sequentially analyzed in order of their best (maximally negative) binding energy viz., atisine, kutkin, phylloquinone, embelin, stigmasterol, convallamarogenin, spinasterol, furostanol, dehydrocostus–lactone, β-sitosterol, amyrin acetate, 4-alpha-Methylcholesta-8,24-dien-3beta-ol (4AMC), lanosterol, erythrodiol, D-friedoolean-14-en-3-one, 6-acetonyldihydrochelerythrine, lupeol, verazine, protopine, nuciferine, dihydrosanguinarine, cadiyenol, picrinine, 1H-Indole-2,3-dione, 5-pentyl-1-(trimethylsilyl)-,3-(O-methyloxime)(1H-ID), maritinone, 6-acetonyldihydroavicine, azadirone,1,2,4-Cyclopentanetrione,3,3-bis(3-methyl-2-butenyl)-5-(3-methyl-1-oxobutyl) (1,2,4-CPT), β-amyrin, epifriedelinol, taraxerol, lyoniresinol, taraxasterol, alschomine, adenanthin, and podophyllotoxin.

The binding energy parameter is one of the most established parameters for evaluating of docking complexes, specifically, protein-small molecule complexes. Since the calculation of binding energy is dependent on the interacting partners, it is difficult to predict an optimum threshold value that can be used as a reference standard universally as the interactions vary based on the partners. The established inhibitors of p-glycoprotein have been used and the binding energies obtained in those interactions have been used to construct the reference range to evaluate the efficacy of the other molecules that have been analyzed.

The lowest binding energy of interaction was observed to be with atisine (-100.76 kcal/mol) and kutkin (-90.8 kcal/mol), components present in *A. heterophyllum*, followed by phylloquinone (-83.13 kcal/mol), a component present in *C. officinalis* (Figure 1).

Table 1. Drug-likeness properties of potential inhibitors

Compounds	MW	LogP	nOHNH	nON	nViolations
Atisine	343.51	3.67	1	3	0
Kutkin	460.44	1.07	4	10	0
Phylloquinone	450.71	8.80	0	2	1
Embelin	294.39	4.62	2	4	0
Stigmasterol	412.70	7.87	1	1	1
Convallamarogenin	430.63	5.04	2	4	1
Spinasterol	412.70	7.87	1	1	1
Furostanol	402.66	6.96	1	2	1
Dehydrocostus lactone	230.31	2.29	0	2	0
Beta-sitosterol	414.72	8.62	1	1	1

MW: Molecular weight; LogP: Log of octanol/water partition coefficient; nON: Number of hydrogen bond acceptors; nOHNH: Number of hydrogen bond donors; nViolations: Number of rule of five violations.

Table 2. Absorption, distribution, metabolism, excretion and toxicity (ADMET) properties of potential inhibitors

Compounds	Water solubility (log mol/L)	CYP P450 2D6 inhibition	Intestinal absorption (% absorbed)	BBB permeability (log BB)	Fraction unbound (Fu)	P-glycoprotein I inhibitor
Atisine	-3.096	Yes	91.762	-0.102	0.322	Yes
Kutkin	-3.639	No	65.029	-1.323	0.1	Yes
Phylloquinone	-6.911	No	96.834	-0.281	0	Yes
Embelin	-4.511	Yes	89.155	-0.06	0.232	Yes
Stigmasterol	-6.682	No	94.97	0.771	0	Yes
Convallamarogenin	-5.23	No	96.482	-0.227	0.02	Yes
Spinasterol	-6.682	No	94.97	0.771	0	Yes
Furostanol	-5.196	No	99.657	0.721	0	Yes
Dehydrocostus lactone	-3.846	No	98.917	0.566	0.268	Yes
Beta-sitosterol	-6.773	No	94.464	0.781	0	Yes

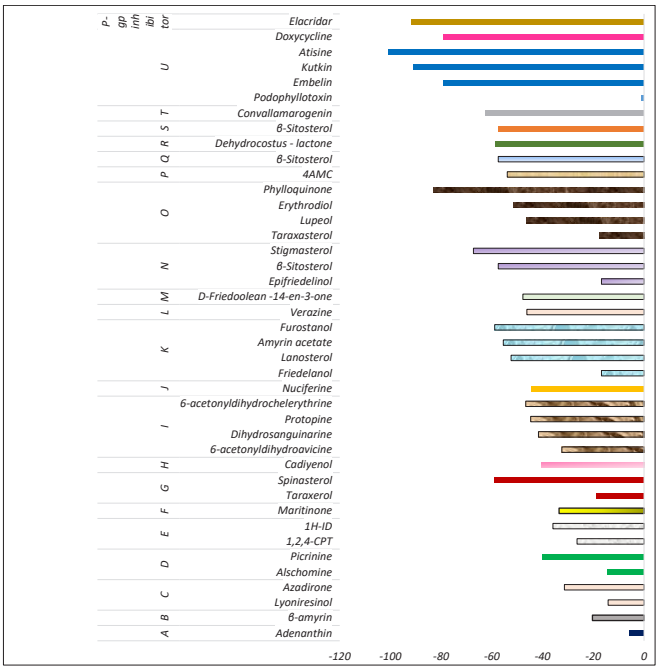

Figure 1. Binding energy of interaction of inhibitory components in reno-protective herbs viz., *(A) Calophyllum inophyllum; (B) Pongamia pinnata; (C) Toona sinensis; (D) Alstonia scholaris; (E) Hypericum mysorense; (F) Plumbago zeylanica; (G) Mimusops elengi; (H) Centella asiatica; (I) Chelidonium majus; (J) Nelumbo nucifera; (K) Ficus bengalensis; (L) Eclipta alba; (M) Pterocarpus marsupium; (N) Paederia foetida; (O) Calendula officinalis; (P) Cocculus pendulus; (Q) Abies webbiana; (R) Saussurea costus; (S) Apium leptophyllum; (T) Convallaria majalis; (U) Aconitum heterophyllum* with doxycycline and elacridar as control.

To assess the selectivity and strength of the receptor-ligand interactions, the hydrogen bonds, and hydrophobic interactions were computed. The analyzed inhibitory components in order of their maximum hydrogen bonded interactions were found to be lyoniresinol, podophyllotoxin, alschomine, atisine, embelin, convallamarogenin, nuciferine, protopine, erythrodiol, picrinine, 6-acetonyldihydroavicine, phylloquinone, 1H-Indole-2,3-dione, 5-pentyl-1-(trimethylsilyl)-,3-(O-methyloxime)(1H-ID), 1,2,4-cyclopentanetrione,3,3-bis(3-methyl-2-butenyl)-5-(3-methyl-1-oxobutyl)(1,2,4-CPT), dehydrocostus–lactone, 4alpha-Methylcholesta-8,24-dien-3beta-ol (4AMC), cadiyenol, maritinone, verazine, spinasterol, and furostanol. Maximal hydrogen bond interactions observed was four, as found in the case of lyoniresinol from *Toona sinensis.* Atisine, a component present in *A. heterophyllum* displayed two hydrogen bond interactions (Figure 2).

The analyzed inhibitory components in order of their maximum hydrophobic interactions were found to be epifriedelinol, friedelanol, amyrin acetate, β-sitosterol, convallamarogenin, D-friedoolean-14-en-3-one, cadiyenol, maritinone, taraxerol, furostanol, 1,2,4-cyclopentanetrione,3,3-bis(3-methyl-2-butenyl)-5-(3-methyl-1-oxobutyl)(1,2,4-CPT), erythrodiol, phylloquinone, spinasterol, 4alpha-Methylcholesta-8,24-dien-3beta-ol (4AMC), verazine, picrinine, dihydrosanguinarine, alschomine, dehydrocostus–lactone, protopine, β-amyrin, 6-acetonyldihydrochelerythrine, azadirone, atisine, kutkin, 1H-indole-2,3-dione, 5-pentyl-1-(trimethylsilyl)-,3-(o-methyloxime)(1H-ID), taraxasterol, lyoniresinol, podophyllotoxin, stigmasterol, lupeol, nuciferine, adenanthin, embelin, and lanosterol. Maximal hydrophobic interaction detected was 10 in epifriedelinol and friedelanol from *Paederia foetida* and *Ficus bengalensis,* respectively. Atisine, a component present in *A. heterophyllum* displayed 6 hydrophobic interactions (Figure S1).

Molecular docking with Discovery Studio (version 2019 onwards) showed that atisine, kutkin, and phylloquinone might serve as the best inhibitors of the efflux transporter. For p-glycoprotein and atisine interaction, two hydrogen bonds were identified with amino acid residues SER979, GLU972, and six hydrophobic (alkyl and pi-alkyl) interactions were observed with PHE72, PHE336, LEU332, LEU975, LEU976, and ILE736. Kutkin, on the other hand, showed six hydrophobic interactions (pi-alkyl, pi-pi T-shaped, pi-pi stacked, and pi-sigma) with PHE336, PHE732, PHE72, LEU975, LEU976, ILE736 at the distance of 5.14 A°, 3.41 A°, 2.83 A°, 5.44 A°, 5.16 A°, and 5.21 A°, respectively. Phylloquinone was involved in one hydrogen bond interaction with LEU332 at the distance of 2.56 A° and eight hydrophobic (pi-pi T-shaped, pi-pi stacked, pi-alkyl, and alkyl) interactions with PHE72, PHE336, PHE732, LEU332, LEU339, LEU975, LEU976, and ILE736 at the distance of 4.43 A°, 5.37 A°, 4.14 A°, 3.41 A°, 5.45 A°, 5.17 A°, 5.43 A°, and 4.71 A°, respectively (Figure 3). Atisine was found to be the best compound among the 376

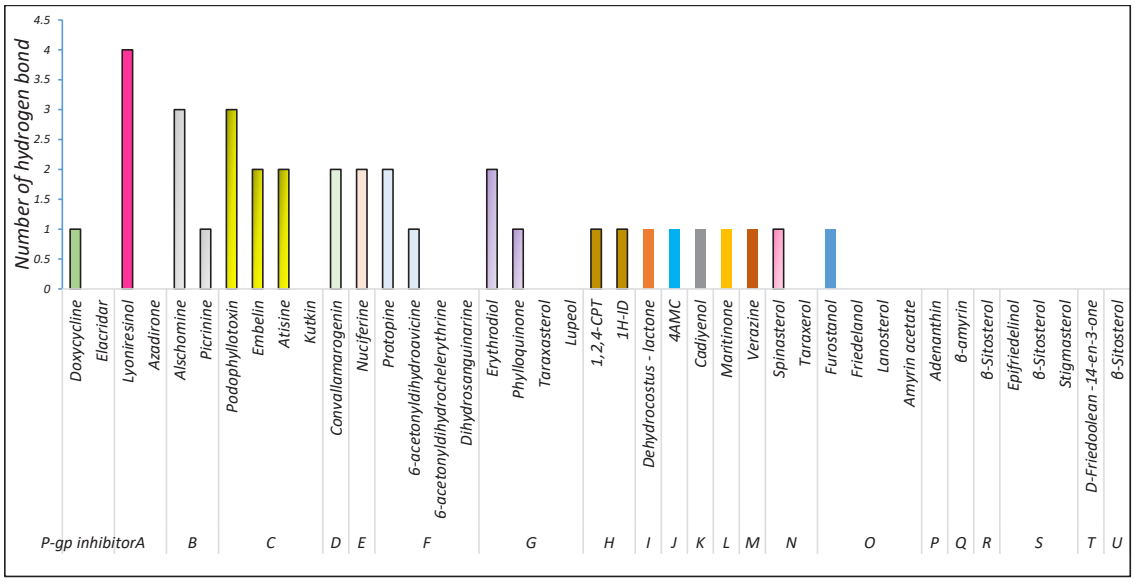

Figure 2. Number of hydrogen bonds of inhibitory components in reno-protective herbs viz., *(A) Toona sinensis; (B) Alstonia scholaris; (C) Aconitum heterophyllum; (D) Convallaria majalis; (E) Nelumbo nucifera; (F) Chelidonium majus; (G) Calendula officinalis; (H) Hypericum mysorense; (I) Saussurea costus; (J) Cocculus pendulus; (K) Centella asiatica; (L) Plumbago zeylanica; (M) Eclipta alba; (N) Mimusops elengi; (O) Ficus bengalensis; (P) Calophyllum inophyllum; (Q) Pongamia pinnata; (R) Apium leptophyllum; (S) Paederia foetida; (T) Pterocarpus marsupium; (U) Abies webbiana* with doxycycline and elacridar as control.

components studied, largely based on binding free energy, along with hydrogen and hydrophobic interactions.

Molecular dynamics simulation

The MD simulation study was conducted using Discovery Studio to predict the efficacy of atisine as possible novel inhibitor. The best pose was obtained from the molecular docking experiment by CDOCKER. The Standard Dynamics Cascade (SDC) performed a series of minimization and equilibration steps followed by molecular dynamics using CHARMm algorithm. SDC summary was acquired from minimization with the steepest descent and conjugate gradient, followed by heating, equilibration and production dynamics. The total energy was found to decrease and the temperature was stable at 301°K±4.

The stability of the conformation was evaluated by a root mean square fluctuation (RMSF) graph. These values were computed to evaluate the effect of the binding of ligands on protein flexibility. The RMSF of a structure is the time average of the RMSD. RMSD quantifies the divergence of a structure from a reference over time while the RSMF can reveal which areas of the system are the most mobile. Though RMSD is frequently calculated to an initial state, the RMSF is calculated to an average structure of the simulation. An area of the structure with high RMSF values frequently diverges from the average, indicating high mobility. Thus, RMSF evaluates the binding poses effectively. In Figure 4, the RMSF graph shows that the structure is not much fluctuating. The key residues viz., SER979, GLU972, LEU332, PHE336, PHE732, LEU975, LEU976, and ILE736 involved in various interactions were found without any abnormal fluctuation and had relatively low RMSF values (0.3-0.6 A°). These findings suggest that the critical interactions of the ligand in the binding pocket might maintain protein stability.

Figure 5 depicts the nature of the binding surface of the protein. The hydrogen bonds are shown by dashed lines. From the figure it can be concluded that one part of the inner pocket is slightly electronegative (Figure 5a) indicated by the small red segment at the base of the surface representation; this can have a positive impact on transient interactions as documented by Pocketome data (40) and acidic (Figure 5e) with a predominance of aromatic residues predominating the core and outer extremities of the pocket (Figure 5b). The binding surface is filled with aromatic residues which contribute to edge interaction and hydrophobicity (Figure 5d). Aromatic stacking has long been recognized as one of the key constituents of ligand-protein interfaces and thus this predominance of aromatic residues indicates that the ligand has found a good fit in the protein neighborhood (41). Several hydrogen bond acceptors and two donors are clearly visible around the bound ligand (Figure 5c). H-bonds are crucial for binding and specificity and other interactions make the structure stable and compact. In biological systems, it has been observed that H-bond competing process is always present with water. Since bulk water interferes with reversible biological processes, enthalpy-entropy compensation occurs during H-bond formation (42). In this study we found that hydrogen bonding was present due to the presence of residues which were potentially hydrophobic in nature and thus this interference was not present here.

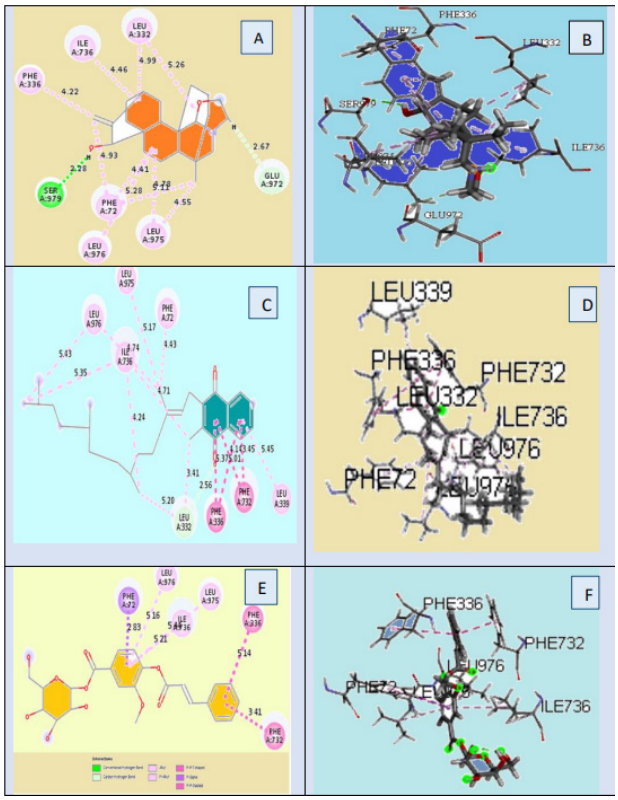

Figure 3. 2D (Left) and 3D (Right) binding poses of inhibitors: Atisine (A-B), phylloquinone (C-D) and kutkin (E-F) with human p-glycoprotein (6C0V). Graphics were generated by CDOCKER.

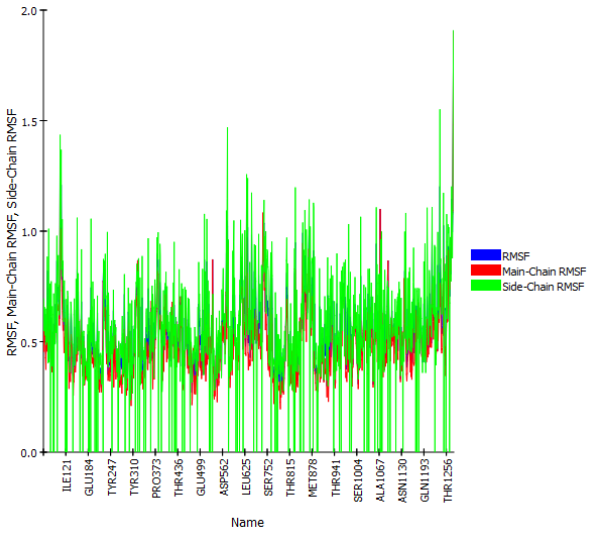

Figure 4. Root-mean-square-fluctuation (RMSF) graph depicting the fluctuation of the residues compared to the average structure across the production trajectory during molecular dynamics simulation.

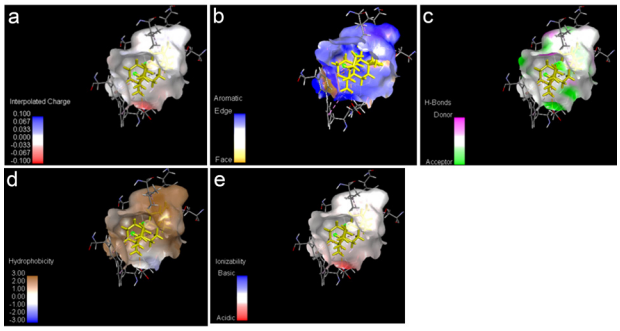

Figure 5. Pocket view of 3D representation of molecular interaction between human p-glycoprotein (6C0V) and atisine: a) binding surface depicting interpolated charge; b) binding surface depicting aromatic residues; c) binding surface and the representation of residues involved in hydrogen bond donor and acceptor; d) hydrophobicity surface representation, and e) ionizability surface representation of p-glycoprotein-atisine complex.

The interaction energy was calculated between sets of atoms across all conformations using CHARMm and was found to be stable. The radius of gyration (Rg) of a protein is computed as the average distance of all atoms to its geometric center: $Rg = (\Sigma r^2)^{1/2} / N$, where r is the distance between an atom and the geometric center and N is the total number of atoms. The radius of gyration is stable around 47.95 Å which shows that the complex structure was compact during simulation.

MM-PBSA method was used to calculate the binding free energy of p-glycoprotein-atisine complex. The binding energy of the protein with the ligand ($G_{binding}$) was calculated for each frame using equation: $G_{binding} = G(a) - G(b) - G(c)$ where, G(a) is the free energy of the protein-ligand complex and G(b) and G(c) are free energies of the protein and ligand, respectively. Then, the average of $G_{binding}$ was calculated over all frames and reported as the DeltaG Average. Average binding free energy (DeltaG Average) was found to be -19.7126 kcal/mol (Table 3). The results of this simulation study showed the stability of the protein-ligand complex and suggested that atisine could likely inhibit p-glycoprotein better than kutkin and phylloquinone.

Discussion

Renal drugs would be partially excreted from the target cells owing to overexpression of the efflux transporter p-glycoprotein. Inhibiting the expulsion by p-glycoprotein would enhance the bioavailability of the desired drugs as there would be retention in the reno-cytes.

Herbal constituents are known to modulate p-glycoprotein activity by directly interacting with the ATP-binding site or the substrate-binding site. Inhibition of the efflux of rhodamine 123 in the MDR human leukaemia cell line by stigmasterol (43) (*Paederia foetida*), the reversion of MDR in NCI/ADR-RES cells by β-Sitosterol (44) (*Abies webbiana*), inhibition of p-glycoprotein mediated efflux of [3H]digoxin in LLCGA5-COL150 cells by lupeol (45) (*C. officinalis*), and p-glycoprotein inhibition in cultured bovine brain capillary endothelial cells by berberine (46) (*A. heterophyllum*) suggest the potency of the bioactive compounds in modulation of p-glycoprotein activity.

Herbal compounds have long been known to promote renal function and slow down the progression of kidney

Table 3. Radius of gyration, interaction energy and binding free energy of all conformations during molecular dynamics simulation

	Time	Radius of Gyration (Å)	VDW Interaction Energy	Electrostatic Interaction Energy	Interaction Energy	G_6C0V_ complex	G_6C0V: B_2	G_not_ 6C0V: B_2	DeltaG_ 6C0V
Conformation 1	16	47.8989	-95.0946	-40.0492	-55.0454	-49739.6	89.0716	-49819.1	-9.5943
Conformation 2	18	47.8655	-81.6751	-41.0953	-40.5798	-49802.3	79.5228	-49868	-13.8354
Conformation 3	20	47.9521	-79.175	-38.1688	-41.0063	-49716.5	80.3239	-49788.5	-8.2759
Conformation 4	22	47.9502	-87.3181	-36.3652	-50.9529	-49896.5	80.6089	-49944.2	-32.9192
Conformation 5	24	47.934	-103.996	-39.0754	-64.9206	-49785	84.5502	-49835.6	-33.9383

disease (47). Berberine (*A. heterophyllum*) has been known to exert reno-protection against gentamicin-induced nephrotoxicity in rats through the attenuation of oxidative stress, apoptosis, and mitochondrial dysfunction (48). Similar reno-conservation effect was observed on the administration of β-sitosterol (*Paederia foetida*) in nephrotoxicity induced in Wistar rats via the up-regulation of Nrf2 gene expression (49). Nuciferine from *Nelumbo nucifera* improved renal injury by the inhibition of TLR4/PI3K/NF-κB signaling pathway and NLRP3 inflammasome activation in rat renal cortex and HK-2 cells (50). So, the simultaneous administration of these natural compounds would not only enhance the accumulation of the renal treatment drugs inside the target cells but also impart additional reno-protection.

The inhibitors of the efflux carrier protein may be sequentially aligned on the basis of their magnitude of negative binding free energy along with hydrogen bonding and hydrophobic interactions, all of which play vital roles in stabilizing the appropriate conformation of the ligand at the target site of the protein. Hydrogen bonding provides directionality and specificity of interaction between the receptor and ligand. The energetics and kinetics of hydrogen bonding need to be optimal thus conferring stability to the protein structure (51). Optimized hydrophobic interactions stabilize the energetically-favored inhibitor ligands at the active sites of the protein and may help alter binding affinity and improve drug efficacy by enhancing the bioavailability in the renal cells.

Doxycycline (52) and elacridar (53) are established inhibitors of p-glycoprotein. Atisine possessed binding energy of -100.76 kcal/mol exceeding the binding energy attained with doxycycline (-79.09 kcal/mol) and elacridar (-91.59 Kcal/mol). Doxycycline was involved in one hydrogen bond (carbon–hydrogen) with LEU976 (3.74 Å) and three hydrophobic interactions (pi-alkyl, alkyl and pi-pi stacked) with residues LEU332 (3.96 Å), ILE736 (4.52 Å) and PHE732 (4.63 Å) at the same binding position. Elacridar was engaged in hydrophobic interactions (one pi-pi stacked, two pi-alkyl, two alkyl) with five residues including PHE732 (5.38 Å), PHE72 (6.80 Å), LEU332 (6.42 Å), ILE328 (5.76 Å), and ALA80 (5.84 Å). Atisine exhibited better binding mode with two hydrogen bond interactions (conventional and carbon–hydrogen) with amino acid residues SER979 (2.28 Å), GLU972 (2.67 Å) and hydrophobic (alkyl and pi-alkyl) interactions with six residues, including PHE72 (4.41 Å), PHE336 (4.22 Å), LEU332 (4.99 Å), LEU975 (4.78 Å), LEU976 (5.28 Å), and ILE736 (4.46 Å). Thus, atisine, a non-toxic (54) active constituent of *A. heterophyllum* with its better binding affinity and stronger interactions than doxycycline and elacridar, maybe considered as the lead compound in circumvention of p-glycoprotein mediated renal drug efflux.

Conclusion

The renoprotective natural compounds which are considered as p-glycoprotein inhibitors, exhibit drug-likeness and other pharmacokinetic attributes. The binding potency of these potential lead compounds promises increased drug bioavailability when co-administered during medical treatment. Hence, atisine is the lead inhibitory component, followed by kutkin and phylloquinone as analyzed from an array of reno-protective herbs which might play significant role in circumvention of drug efflux along with augmentation of renal function. Further *in vitro* and *in vivo* studies are needed to accredit the pharmacological significance of these lead molecules.

Acknowledgement

We would like to express our heartfelt gratitude to West Bengal State University for providing the infrastructural facilities to pursue our studies. We are also grateful to Dr Atreyee Mukherjee for editing the English language.

Authors' contribution

PG conceptualized; CR performed the data collection, analysis, validation, and preparation; PG and CR supported during the validation and preparation of the final manuscript. All authors read, reviewed, and approved the manuscript and edited English language.

Conflict of interest

The authors declare that there is no conflict of interest.

Ethical considerations

The manuscript is not submitted to or being considered by another journal in part or full for publication. No part of the manuscript contains plagiarized portion from any other published material.

Funding/Support

The software and essentials were partially provided from the general RUSA fund of West Bengal State University.

Supplementary files

Supplementary file 1 contains Table S1 and Figure S1.

References

1. Edwards JE, Alcorn J, Savolainen J, Anderson BD, McNamara PJ. Role of P-glycoprotein in distribution of nelfinavir across the blood-mammary tissue barrier and blood-brain barrier. Antimicrob Agents Chemother. 2005;49(4):1626-8. doi: 10.1128/aac.49.4.1626-1628.2005.
2. Khan MA, Kassianos AJ, Hoy WE, Alam AK, Healy HG, Gobe GC. Promoting plant-based therapies for chronic kidney disease. J Evid Based Integr Med. 2022;27:2515690x221079688. doi:10.1177/2515690x221079688.
3. Sabiu S, O'Neill FH, Ashafa AOT The purview of phytotherapy in the management of kidney disorders: a systematic review on Nigeria and South Africa. Afr J Tradit Complement Altern Med. 2016;13(5):38-47. doi: 10.21010/ajtcam.v13i5.6.
4. Ganesan M, Kanimozhi G, Pradhapsingh B, Khan HA, Alhomida AS, Ekhzaimy A, et al. Phytochemicals reverse P-glycoprotein mediated multidrug resistance via signal transduction pathways. Biomed Pharmacother. 2021;139:111632. doi: 10.1016/j.biopha.2021.111632.
5. Anglicheau D, Pallet N, Rabant M, Marquet P, Cassinat B, Méria P, et al. Role of P-glycoprotein in cyclosporine cytotoxicity in the cyclosporine-sirolimus interaction. Kidney Int. 2006;70(6):1019-25. doi: 10.1038/sj.ki.5001649.
6. Wang J, Figurski M, Shaw LM, Burckart GJ. The impact of P-glycoprotein and Mrp2 on mycophenolic acid levels in mice. Transpl Immunol. 2008;19(3-4):192-6. doi: 10.1016/j.trim.2008.05.009.
7. Jeong H, Chiou WL. Role of P-glycoprotein in the hepatic metabolism of tacrolimus. Xenobiotica. 2006;36(1):1-13. doi: 10.1080/00498250500485115.
8. Obermeier M, Yao M, Khanna A, Koplowitz B, Zhu M, Li W, et al. In vitro characterization and pharmacokinetics of dapagliflozin (BMS-512148), a potent sodium-glucose cotransporter type II inhibitor, in animals and humans. Drug Metab Dispos. 2010;38(3):405-14. doi: 10.1124/dmd.109.029165.
9. Goo YT, Song SH, Yeom DW, Chae BR, Yoon HY, Kim CH, et al. Enhanced oral bioavailability of valsartan in rats using a supersaturable self-microemulsifying drug delivery system with P-glycoprotein inhibitors. Pharm Dev Technol. 2020;25(2):178-86. doi: 10.1080/10837450.2019.1683749.
10. Dhalwal K, Deshpande YS, Purohit AP. Evaluation of in vitro antioxidant activity of *Sida rhombifolia* (L.) ssp. *retusa* (L.). J Med Food. 2007;10(4):683-8. doi: 10.1089/jmf.2006.129.
11. Morris S, Jha AK, Swarnakar Y. Phytochemical screening of plant *Apium leptophyllum* seeds. Int J Nanomater Nanotechnol Nanomed. 2015;203.
12. Konda VG, Eerike M, Raghuraman LP, Rajamanickam MK. Antioxidant and nephroprotective activities of *Aconitum heterophyllum* root in glycerol induced acute renal failure in rats. J Clin Diagn Res. 2016;10(3):FF01-2. doi: 10.7860/jcdr/2016/10798.7388.
13. Rajalakshmi P, Vadivel V, Ravichandran N, Sudha V, Brindha P. Pharmacognostic evaluation of *Abies webbiana* leaf: a Siddha herbal ingredient. Asian J Pharm Clin Res. 2016;9(4):213-9.
14. Azeem AK, Rasheed A, Dilip C, Junise V, Rani S. Diuretic activity of the fruits of *Artocarpus hirsutus* Lam. J Curr Sci. 2013;1(1):16-9.
15. Borgohain MP, Chowdhury L, Ahmed S, Bolshette N, Devasani K, Das TJ, et al. Renoprotective and antioxidative effects of methanolic *Paederia foetida* leaf extract on experimental diabetic nephropathy in rats. J Ethnopharmacol. 2017;198:451-9. doi: 10.1016/j.jep.2017.01.035.
16. Jangir S, Mathur K, Goyal M, Yadav SK. A Review on *Cocculus pendulus* (J.R. Forst. & G. Forst.) diels: traditional uses, phytochemistry and pharmacological properties. Indian J Drugs. 2016;4(2):57-62.
17. Geetha K, Ramarao N. Nephroprotective and nephrocurative activity of *Alangium salvifolium* against gentamicin induced nephrotoxicity in albino rats. J Pharm Res. 2014;8(9):1248-55.
18. Hussein OE, Germoush MO, Mahmoud AM. *Ruta graveolens* protects against isoniazid/rifampicin-induced nephrotoxicity through modulation of oxidative stress and inflammation. Glob J Biotechnol Biomater Sci. 2016;2(1):8-13.
19. Shanmugapriya, Chen Y, Jothy SL, Sasidharan S. *Calophyllum inophyllum*: a medical plant with multiple curative values. Res J Pharm Biol Chem Sci. 2016;7(4):1446-52.
20. Divakar K, Pawar AT, Chandrasekhar SB, Dighe SB, Divakar G. Protective effect of the hydro-alcoholic extract of *Rubia cordifolia* roots against ethylene glycol induced urolithiasis in rats. Food Chem Toxicol. 2010;48(4):1013-8. doi: 10.1016/j.fct.2010.01.011.
21. Yılmaz H, Ekinci N, Ömerli A, Nisari M, Yay AH, Ülger H, et al. The protective effect of *Myrtus communis* L. against experimental kidney stone in rats. Adv Tradit Med. 2022. doi: 10.1007/s13596-021-00620-4.
22. Shirwaikar A, Malini S, Kumari SC. Protective effect of *Pongamia pinnata* flowers against cisplatin and gentamicin induced nephrotoxicity in rats. Indian J Exp Biol. 2003;41(1):58-62.
23. Lateef T, Rukash H, Bibi F, Azmi MB, Qureshi SA. Effect of *Convallaria majalis* on kidney function. J Dow Univ Health Sci. 2010;4(3):94-7.
24. Ashry M, Galal El-Sahra D, Gaber DA, M AM, Abdel-Wahhab KG. Nephroprotective effect of costus (*Saussurea costus*) ethanolic extract on oxaliplatin®-induced nephrotoxicity in adult male Wistar rats. Pak J Biol Sci. 2021;24(8):830-9. doi: 10.3923/pjbs.2021.830.839.
25. Katedeshmukh RG, Shete RV, Otari KV, Bagade MY, Pattewar A. Acute toxicity and diuretic activity of *Mimusops elengi* extracts. Int J Pharma Bio Sci. 2010;1(3):1-6.
26. Preethi KC, Kuttan R. Hepato and reno protective action of *Calendula officinalis* L. flower extract. Indian J Exp Biol. 2009;47(3):163-8.
27. Yadav YC. Effect of *Ficus benghalensis* L. latex extract (FBLE) on cisplatin induced hypotension and renal impairment in

Wistar rats. Biochem Pharmacol (Los Angel). 2016;5(4):216. doi: 10.4172/2167-0501.1000216.
28. Gopinath S, Sakthidevi G, Muthukumaraswamya S, Mohan VR. GC-MS analysis of bioactive constituents of *Hypericum mysorense* (Hypericaceae). J Curr Chem Pharm Sci. 2013;3(1):6-15.
29. Li WZ, Wang XH, Zhang HX, Mao SM, Zhao CZ. Protective effect of the n-butanol *Toona sinensis* seed extract on diabetic nephropathy rat kidneys. Genet Mol Res. 2016;15(1). doi: 10.4238/gmr.15017403.
30. Dubey T, Srivastava AK, Nagar H, Mishra BK, Mishra SS. Nephroprotective activity of *Nelumbo nucifera* Gaertn. roots, leaves and flowers on gentamicin induced nephrotoxicity. Asian J Pharm Educ Res. 2014;3(4):134-51.
31. Koriem KM, Arbid MS, Asaad GF. *Chelidonium majus* leaves methanol extract and its chelidonine alkaloid ingredient reduce cadmium-induced nephrotoxicity in rats. J Nat Med. 2013;67(1):159-67. doi: 10.1007/s11418-012-0667-6.
32. Dungca NT. Protective effect of the methanolic leaf extract of *Eclipta alba* (L.) Hassk. (Asteraceae) against gentamicin-induced nephrotoxicity in Sprague Dawley rats. J Ethnopharmacol. 2016;184:18-21. doi: 10.1016/j.jep.2016.03.002.
33. Bharati D, Goyal S, Bose A. Nephroprotective activity of dichloromethane extract of leaves of *Alstonia scholaris* Linn. in gentamycin induced nephrotoxicity in rats: preventive study. Res J Pharm Technol. 2021;14(2):1055-8. doi: 10.5958/0974-360x.2021.00189.x.
34. Gupta P, Sharma P, Shanno K, Jain V, Pareek A, Agarwal P, et al. Nephroprotective role of alcoholic extract of *Pterocarpus marsupium* heartwood against experimentally induced diabetic nephropathy. J Pharm Pharmacogn Res. 2016;4(5):174-86.
35. Setyaningsih WAW, Arfian N, Fitriawan AS, Yuniartha R, Sari DCR. Ethanolic extract of *Centella asiatica* treatment in the early stage of hyperglycemia condition inhibits glomerular injury and vascular remodeling in diabetic rat model. Evid Based Complement Alternat Med. 2021;2021:6671130. doi: 10.1155/2021/6671130.
36. Rajakrishnan R, Lekshmi R, Benil PB, Thomas J, Alfarhan AH, Rakesh V, et al. Phytochemical evaluation of roots of *Plumbago zeylanica* L. and assessment of its potential as a nephroprotective agent. Saudi J Biol Sci. 2017;24(4):760-6. doi: 10.1016/j.sjbs.2017.01.001.
37. Kim Y, Chen J. Molecular structure of human P-glycoprotein in the ATP-bound, outward-facing conformation. Science. 2018;359(6378):915-9. doi: 10.1126/science.aar7389.
38. Lipinski CA, Lombardo F, Dominy BW, Feeney PJ. Experimental and computational approaches to estimate solubility and permeability in drug discovery and development settings. Adv Drug Deliv Rev. 2001;46(1-3):3-26. doi: 10.1016/s0169-409x(00)00129-0.
39. Pires DE, Blundell TL, Ascher DB. pkCSM: predicting small-molecule pharmacokinetic and toxicity properties using graph-based signatures. J Med Chem. 2015;58(9):4066-72. doi: 10.1021/acs.jmedchem.5b00104.
40. Kufareva I, Chen YC, Ilatovskiy AV, Abagyan R. Compound activity prediction using models of binding pockets or ligand properties in 3D. Curr Top Med Chem. 2012;12(17):1869-82. doi: 10.2174/156802612804547335.
41. Brylinski M. Aromatic interactions at the ligand-protein interface: implications for the development of docking scoring functions. Chem Biol Drug Des. 2018;91(2):380-90. doi: 10.1111/cbdd.13084.
42. Chen D, Oezguen N, Urvil P, Ferguson C, Dann SM, Savidge TC. Regulation of protein-ligand binding affinity by hydrogen bond pairing. Sci Adv. 2016;2(3):e1501240. doi: 10.1126/sciadv.1501240.
43. El-Readi MZ, Hamdan D, Farrag N, El-Shazly A, Wink M. Inhibition of P-glycoprotein activity by limonin and other secondary metabolites from *Citrus* species in human colon and leukaemia cell lines. Eur J Pharmacol. 2010;626(2-3):139-45. doi: 10.1016/j.ejphar.2009.09.040.
44. Rubis B, Polrolniczak A, Knula H, Potapinska O, Kaczmarek M, Rybczynska M. Phytosterols in physiological concentrations target multidrug resistant cancer cells. Med Chem. 2010;6(4):184-90. doi: 10.2174/1573406411006040184.
45. Dewanjee S, Dua TK, Bhattacharjee N, Das A, Gangopadhyay M, Khanra R, et al. Natural products as alternative choices for P-glycoprotein (P-gp) inhibition. Molecules. 2017;22(6):871. doi: 10.3390/molecules22060871.
46. He L, Liu GQ. Effects of various principles from Chinese herbal medicine on rhodamine123 accumulation in brain capillary endothelial cells. Acta Pharmacol Sin. 2002;23(7):591-6.
47. Zhong Y, Menon MC, Deng Y, Chen Y, He JC. Recent advances in traditional Chinese medicine for kidney disease. Am J Kidney Dis. 2015;66(3):513-22. doi: 10.1053/j.ajkd.2015.04.013.
48. Adil M, Kandhare AD, Dalvi G, Ghosh P, Venkata S, Raygude KS, et al. Ameliorative effect of berberine against gentamicin-induced nephrotoxicity in rats via attenuation of oxidative stress, inflammation, apoptosis and mitochondrial dysfunction. Ren Fail. 2016;38(6):996-1006. doi: 10.3109/0886022x.2016.1165120.
49. Sharmila R, Sindhu G, Arockianathan PM. Nephroprotective effect of β-sitosterol on N-diethylnitrosamine initiated and ferric nitrilotriacetate promoted acute nephrotoxicity in Wistar rats. J Basic Clin Physiol Pharmacol. 2016;27(5):473-82. doi: 10.1515/jbcpp-2015-0085.
50. Wang MX, Zhao XJ, Chen TY, Liu YL, Jiao RQ, Zhang JH, et al. Nuciferine alleviates renal injury by inhibiting inflammatory responses in fructose-fed rats. J Agric Food Chem. 2016;64(42):7899-910. doi: 10.1021/acs.jafc.6b03031.
51. Hubbard RE, Haider MK. Hydrogen bonds in proteins: role and strength. In: Encyclopedia of Life Sciences (ELS). Chichester: John Wiley & Sons; 2010. doi: 10.1002/9780470015902.a0003011.pub2.
52. Agbedanu PN, Anderson KL, Brewer MT, Carlson SA. Doxycycline as an inhibitor of p-glycoprotein in the alpaca for the purpose of maintaining avermectins in the CNS during treatment for parelaphostrongylosis. Vet Parasitol. 2015;212(3-4):303-7. doi: 10.1016/j.vetpar.2015.09.002.
53. Rowbottom C, Pietrasiewicz A, Tuczewycz T, Grater R, Qiu D, Kapadnis S, et al. Optimization of dose and route of administration of the P-glycoprotein inhibitor, valspodar (PSC-833) and the P-glycoprotein and breast cancer resistance protein dual-inhibitor, elacridar (GF120918) as dual infusion in rats. Pharmacol Res Perspect. 2021;9(2):e00740. doi: 10.1002/prp2.740.
54. Malhotra N, Kumar V, Sood H, Singh TR, Chauhan RS. Multiple genes of mevalonate and non-mevalonate pathways contribute to high aconites content in an endangered medicinal herb, *Aconitum heterophyllum* Wall. Phytochemistry. 2014;108:26-34. doi: 10.1016/j.phytochem.2014.08.025.